ACS APPLIED MATERIALS & INTERFACES

RESEARCH ARTICLE

www.acsami.org

Polyimide Aerogels Cross-Linked through Amine Functionalized Polyoligomeric Silsesquioxane

Haiquan Guo,[*,†] Mary Ann B. Meador,[*,‡] Linda McCorkle,[†] Derek J. Quade,[‡] Jiao Guo,[§] Bart Hamilton,[§] Miko Cakmak,[§] and Guilherme Sprowl[‡]

[†]Ohio Aerospace Institute, 22800 Cedar Point Road, Cleveland, Ohio, United States

[‡]NASA Glenn Research Center, 21000 Brookpark Road, Cleveland, Ohio 44135, United States

[§]National Polymer Innovation Center, The University of Akron, Akron, Ohio 44325, United States

ABSTRACT: We report the first synthesis of polyimide aerogels cross-linked through a polyhedral oligomeric silsesquioxane, octa-(aminophenyl)silsesquioxane (OAPS). Gels formed from polyamic acid solutions of 3,3′,4,4′-biphenyltetracarboxylic dianhydride (BPDA), bisaniline-p-xylidene (BAX) and OAPS were chemically imidized and dried using supercritical CO_2 extraction to give aerogels having density around 0.1 g/cm^3. The aerogels are greater than 90 % porous, have high surface areas (230 to 280 m^2/g) and low thermal conductivity (14 mW/m-K at room temperature). Notably, the polyimide aerogels cross-linked with OAPS have higher modulus than polymer reinforced silica aerogels of similar density and can be fabricated as both monoliths and thin films. Thin films of the aerogel are flexible and foldable making them an ideal insulation for space suits, and inflatable structures for habitats or decelerators for planetary re-entry, as well as more down to earth applications.

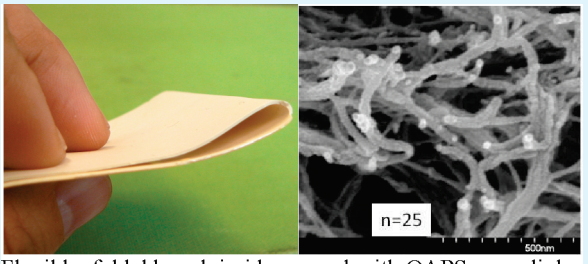

Flexible, foldable polyimide aerogel with OAPS cross-links

KEYWORDS: aerogels, polyimides, polyoligomeric silsesquioxane, mesoporous

INTRODUCTION

An aerogel is a porous solid made by removing the solvent from a gel, typically by supercritical fluid extraction, while maintaining the porosity of the solid network structure.[1] Due to the low density, high porosity and small pore size, aerogels are of interest for many applications including thermal insulation, optics, acoustic insulation and catalysis.[2,3] Although silica aerogels are the most widely studied, potential applications of silica aerogel monoliths in aerospace, industry, and daily life have been restricted because of their poor mechanical properties and hygroscopic nature.[4−6] Hence, monolithic silica aerogels have been limited to exotic applications such as collecting comet dust particles in the NASA Stardust Mission,[7] and as thermal insulation for the batteries and electronics on the Mars Rover.[8]

It has been shown that mechanical properties of silica aerogels can be greatly improved by reacting oligomers such as isocyanate,[9−12] epoxy,[13−15] styrene[16,17] and cyanoacrylates[18] with hydroxyl, amines, or vinyl groups on the silica surface to reinforce the structure. However, the use temperature of these polymer reinforced silica aerogels is limited by the type of polymer reinforcement used, and is well below 200 °C for those previously reported. For many aerospace applications, such as insulation for launch vehicles or inflatable decelerators for entry, descent, and landing applications (EDL), much higher use temperatures are needed. In particular, EDL applications require flexible, even foldable, insulation with high-temperature performance.[19,20] Inflatable decelerators for EDL applications need to stow in a small space and deploy into a large area lightweight heat shield to survive reentry. Minimizing weight and thickness of the system as well as providing suitable insulation are important considerations.

Polyimides are widely used as matrix resins for fiber-reinforced composites for aircraft engine applications because of their high temperature stability. Previously, linear polyimide aerogels (no silica) made from aromatic dianhydrides and diamines, have been reported.[21,22] Though mechanical properties for these aerogels are as good as previously reported polymer reinforced aerogels of similar density, they tend to exhibit a large amount of shrinkage during the fabrication process. More recently, polyimide aerogels cross-linked through aromatic triamines have been synthesized.[23,24] Gelation of the polyimides occurred upon cooling after thermal imidization in glass molds. Supercritical fluid extraction of the gels produced polyimide aerogels from certain formulations with very little shrinkage and up to 90% porosity.

In this study, we report the use of octa(aminophenyl)silsesquioxane (OAPS) to cross-link polyimides in solution to create polyimide aerogels. OAPS is a nanoscale polyhedral oligomeric silsesquioxane cage structure consisting of a silicon and oxygen framework with eight aminophenyl groups attached.[25] Such cage structures with various reactive groups can be incorporated into polymers to improve thermal and mechanical properties,[26,27] dielectric properties,[28] atomic oxygen resistance, and abrasion

Received: November 16, 2010
Accepted: January 17, 2011
Published: February 4, 2011

ACS Publications © 2011 American Chemical Society

Scheme 1. Synthesis of Polyimide Aerogels Cross-Linked with OAPS where *n* is the Number of Repeat Units in BPDA and BAX Oligomers

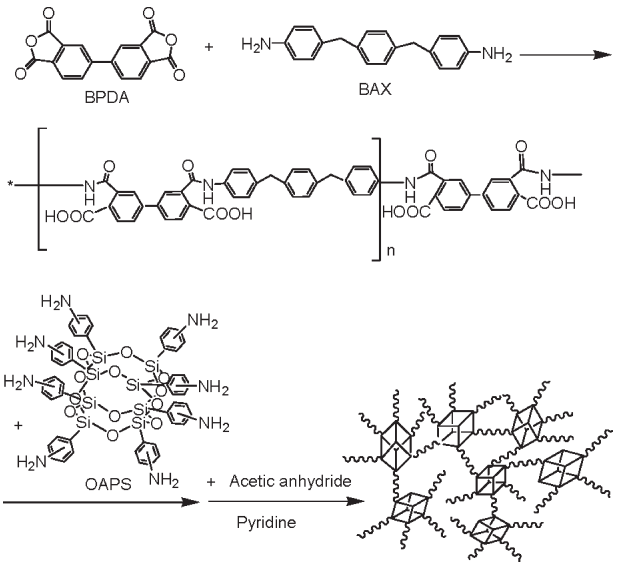

resistance.[29] Polyimide nanocomposites fabricated from OAPS show enhancements in thermal and mechanical properties of polyimide.[30−33] In this study, as shown in Scheme 1, OAPS is used to form a cross-linked poly(amic acid) by reacting with the terminal anhydride groups of oligomers made from 3,3′,4,4′-biphenyltetracarboxylic dianhydride (BPDA) and bisaniline-p-xylidene (BAX). The oligomers are formulated with repeat units, n, of 10, 15, 20, and 25 as shown in Scheme 1. BPDA and BAX are typical monomers used in polyimide matrix resins for high-temperature applications. BPDA is known to impart high temperature stability, high glass-transition temperatures, and better processability to polyimides.[34] BAX was developed as a less toxic replacement for 4,4-methylenedianiline which is a component in PMR-15, a widely used polyimide matrix resin for composites for high temperature aircraft engine applications.[35] Using pyridine to catalyze imidization and acetic anhydride to scavenge water byproduct of the condensation, polyimide gels are obtained. Supercritical fluid extraction using CO_2 produces polyimide aerogels with very little shrinkage. Fabrication of both molded cylinders and highly flexible, thin film polyimide aerogel monoliths is demonstrated. Mechanical and thermal properties of the aerogels will be discussed and related to morphology and chemical structure.

EXPERIMENTAL SECTION

Materials. BPDA was purchased from Chriskev, Inc, (13920 W 108th Street, Lenexa, Kansas, 66215, USA). BAX was obtained from Maverick, Inc, (11379 Grooms Road, Cincinnati, OH 45242-14050). OAPS as a mixture of isomers (meta:ortho:para = 60:30:10) was acquired from Gelest, Inc. An all para-isomer, p-OAPS was purchased from Hybrid Plastic, Inc. HPLC grade N-methyl-2-pyrrolidinone (NMP) and pyridine were purchased from Sigma-Aldrich. Anhydrous acetic anhydride was purchased from Fisher Scientific. All reagents were used without further purification.

General. Attenuated total reflectance (ATR) infrared spectroscopy was conducted using a Nicolet Nexus 470 FT-IR spectrometer. Solid ^{13}C NMR spectroscopy was carried out with a Bruker Avance-300 spectrometer, using cross-polarization and magic angle spinning at 11 kHz. The solid ^{13}C spectra were externally referenced to the carbonyl of glycine (176.1 relative to tetramethylsilane, TMS). Scanning electron micrographs were obtained using a Hitachi S-4700 Field Emission Microscope after sputter coating the samples with gold. The samples were out-gassed at 80°C for 8 h under vacuum before running nitrogen-adsorption porosimetry with an ASAP 2000 Surface Area/Pore Distribution Analyzer (Micromeritics Instrument Corp.). The skeletal density was measured using a Micromeritics Accupyc 1340 Helium Pycnometer. Thermal gravimetric analysis (TGA) was performed using a TA model 2950 HiRes instrument. Samples were run at a temperature ramp rate of 10 °C per min from room temperature to 750 °C under nitrogen or air.

Preparation of OAPS Cross-Linked Polyimide Aerogel Monoliths. Polyamic acid oligomer was formulated in NMP using a molar ratio of BPDA: BAX of $(n + 1)$:*n*, where *n* is the number of repeat units in the oligomers capped with anhydride as shown in Scheme 1. Because each OAPS contains eight amine groups that can react with polyamic acid oligomers, a ratio of four oligomers to one OAPS was used. The total weight of precursors in solution was formulated to be 10 w/w % in all cases. A sample procedure for $n = 25$ oligomer is as follows: To a solution of BAX (1.204 g, 4.18 mmol) in 19 mL of NMP was added BPDA (1.278 g, 4.34 mmol). The mixture was stirred until all BPDA was dissolved, after which a solution of OAPS (0.0481 g, 0.042 mmole) in 3.15 mL of NMP was added. The resulting solution was stirred for 10 min, after which acetic anhydride (3.275 mL, 34.7 mmol) and then pyridine (2.81 mL, 34.7 mmol) were added, both representing an eight to one ratio of acetic anhydride to BPDA. The sol solution was continually stirred for 10 min and then poured into a 20 mL syringe mold (2 cm in diameter), prepared by cutting off the needle end of the syringe and extending the plunger all the way out. Gelation took place within 60 min. The gel was aged in the mold for one day before extracting into NMP where it soaked for 24 h to remove acetic acid and pyridine. The solvent within the gels was then gradually exchanged to acetone in 24 h intervals starting with 75% NMP in acetone, followed by 25% NMP in acetone and finally 100% acetone. The gels were then placed in a 1 L supercritical fluid extraction chamber in acetone, and washed with liquid CO_2 at ∼100 Bar and ∼25 °C in four two-hour cycles. The chamber was then heated to 45 °C and the CO_2 was converted into a supercritical state. Gaseous CO_2 was slowly vented out at the rate 4.5 m/h from the chamber over three hours. The dry polyimide aerogels produced in this way have a density of 0.108 g/cm^3 and porosity of 92%. ^{13}C CP-MAS NMR δ 40, 126, 138, 165; FTIR: 1775 (m), 1715 (s), 1510 (m), 1370 (s) cm^{-1}.

Procedure to Make Polyimide Aerogel Films. The same OAPS cross-linked polyamic acid solution as described above was poured into a 6 inch wide Doctor blade with 0.762 mm gap, and cast onto a Kapton carrier film at a speed of 20 cm/min. The film which gelled within sixty minutes was peeled away from the Kapton under acetone. Afterwards, the films were washed in 24 h intervals in 75% NMP in acetone, followed by 25 % NMP in acetone and finally washed three more times with acetone. Supercritical drying was carried out as described before to give polyimide aerogel thin films with similar properties to above.

Mechanical Characterization. The specimens were cut and polished to make sure that the top and bottom surfaces were smooth and parallel. The diameter and length of the specimens were measured before testing. ASTM standard D695-02a (Compressive Properties of Rigid Plastics) was used as the guideline for this series of testing. Because of the rapid rate of buckling seen in aerogels, the sample lengths were smaller than the ASTM standard (varying between lengths of 0.5 and 1.0 inches). Samples were conditioned at room temperature for 48 h prior to testing. The samples were tested between a pair of compression plates on a Model 4505 Instron load frame using Series IX data

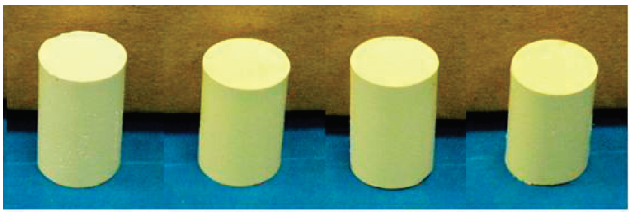

Figure 1. OAPS cross-linked polyimide aerogels made from, left to right, $n = 25$, $n = 20$, $n = 15$, and $n = 10$ oligomers.

acquisition software. All testing was done at nominal room conditions, and at a separation rate of 0.05 in/min as dictated by the ASTM guidelines. The Young's modulus was taken as the initial slope from the stress strain curve of the compression.

Thermal Physical Property Testing of Polyimide Aerogel Film. The thin films were measured at the Thermophysical Properties Research Lab, Inc., located at 3080 Kent Avenue, West Lafayette, IN 47906. The step heating (3P) method was used which involves subjecting one face of a specimen to a uniform heat flux and recording the temperature responses at various locations.[36] A 60 W light bulb, mounted within an aluminum parabolic reflector, is the heat flux source. Temperature rise curves are measured at three locations using K-type thermocouples spaced along the sample. The two outside locations (one on each end) are used as boundary conditions and interior position data are used as the basis for the diffusivity calculations. Specific heat is measured using a standard Perkin-Elmer Model DSC-2 Differential Scanning Calorimeter with sapphire as the reference material (ASTM E1269). The standard and sample were subjected to the same heat flow as a blank and the differential powers required to heat the sample and standard at the same rate were determined using the digital data acquisition system. From the masses of the sapphire standard and sample, the differential power, and the known specific heat of sapphire, the specific heat of the sample is computed. All measured quantities are directly traceable to NIST standards. Before the diffusivity measurement, the samples were kept in vacuum chamber for at least 20 min in order to dry the sample material. The chamber was then flushed twice and finally filled with dry nitrogen gas at normal pressure $p = 760$ Torr. The sample temperature was measured using three K-type thermocouples (4 mils wire thickness) welded separately to thin stainless steel foils of dimensions 8 mm $\times$8 mm $\times$0.062 mm, with oxidized surfaces. Test specimens consisted of four layers of polyimide aerogel thin films. No opacifiers were used. The composite specimen used for the diffusivity measurement had a average bulk density $\rho_b = 0.121$ g/cm^3, 5 cm diameter, thickness of 0.3759 cm, and mass of 0.8915 g. Total relative expanded uncertainty (coverage factor $k = 2$) of the density measurement is $\pm$3%. Total relative expanded uncertainty ($k = 2$) of the specific heat measurement is $\pm$3%.

RESULTS AND DISCUSSION

Polyimide aerogels were made using 10 w/w % solution of OAPS, BPDA and BAX, in NMP, with the formulated number of repeat units, n, ranging from 10 to 25. Amber colored polyamic acid oligomers with terminal anhydride groups are formed in solution from (n + 1) equivalents of BPDA and n equivalents of BAX upon mixing, as shown in Scheme 1. The terminal anhydride groups react with the amines of OAPS, after which pyridine (to catalyze imidization) and acetic anhydride (to scavenge water byproduct of condensation) are added to the solution. Gelation occurs in 30 minutes to one hour, with longer oligomers requiring the longest gel time. All of the samples from the study are light yellow and opaque as shown in Figure 1 for $n = 25$ samples. Shrinkage of the aerogels during fabrication is minimal, ranging

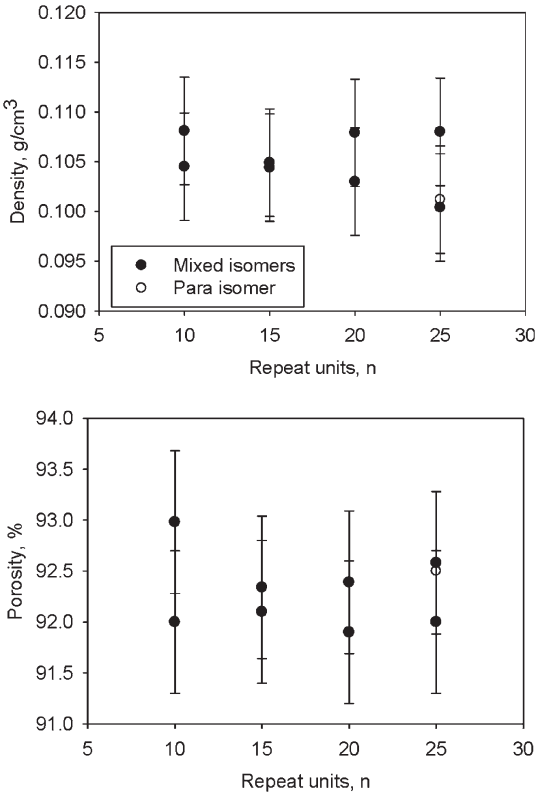

Figure 2. Density and porosity of aerogels graphed vs number of repeat units, *n*.

from 11−13%, measured as the difference between the diameter of the mold and the dried samples.

As reported by Laine et al,[24] ^{29}Si NMR of OAPS in solution contains two peaks at −73.3 and −77.4 ppm. Solid ^{29}Si NMR of the polyimide aerogels fabricated in this study show a broad resonance at −75 ppm, characteristic of the polysilsesquioxane structure. Solid ^{13}C NMR spectra of the aerogels have the expected broad peaks 40 ppm (methylenes from BAX), 126 ppm and 138 ppm (aromatic carbons), and 165 ppm (imide carbonyl). FTIR spectra also contain characteristic bands for polyimide at 1370 cm^{-1} (υ imide C−N), 1715 cm^{-1} (symmetric υ imide C═O) and 1775 cm^{-1} (asymmetric υ imide C═O). A band at ∼1860 cm^{-1}, which would indicate the existence of unreacted anhydride, is not observed. In addition, bands at ∼1660 cm^{-1} (υ amic acid C═O) and ∼1535 cm^{-1} (υ amide C−N) are absent, further indicating that imidization is complete. Bands at ∼1807 and 980 cm^{-1} expected for the isoimide structure also are not observed in the FTIR spectra.

The densities of the polyimide aerogels all fall between 0.10 to 0.11 g/cm^3 as seen in Figure 2, with no difference seen for number of repeat units between cross-links. Using bulk density (ρ_b) and skeletal density (ρ_s) measured by helium pycnometry, the percent porosity can be calculated using eq 1

$$\text{porosity} = (1 - \rho_b / \rho_s) \times 100\% \qquad (1)$$

Again as shown in Figure 2, no effect of the number of repeat units is seen on porosity which ranged from 91 to 92% for all aerogels studied. In addition, use of OAPS as a mixture of isomers (black circles in Figure 2) for cross-linking vs *p*-OAPS (open circles) also appears to have no effect on density and porosity.

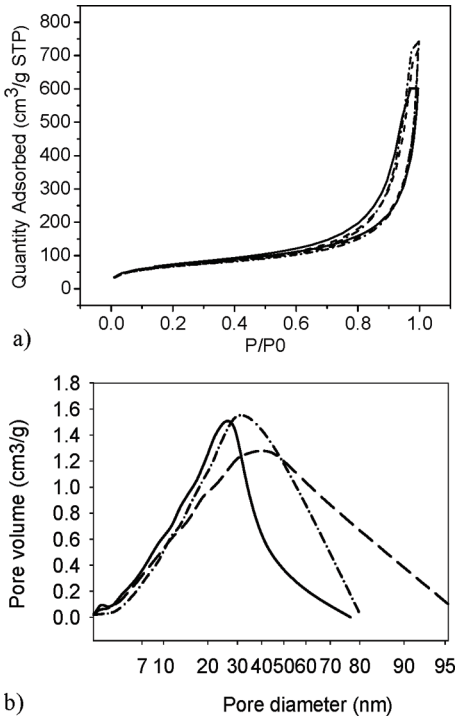

Figure 3. (a) Typical N_2 adsorption−desorption isotherms (at 77 K), and (b) graph of relative pore volume vs pore diameter of the polyimide aerogel $n = 10$ (dotted line), $n = 15$ (dash line), $n = 20$ (dash-dotted line) and $n = 25$ (solid line).

The surface areas and pore volume of the monoliths were measured by nitrogen sorption using the Branuaer−Emmet−Teller (BET) method. The BET surface areas of the samples are in the range of 240−260 m^2/g again independent of number of repeat units or the OAPS isomer used. Typical nitrogen adsorption and desorption isotherms at 77 K for of the monoliths are shown in Figure 3. IUPAC conventions have been developed to classify gas sorption isotherms and their relationship to the porosity of materials.[37] In Figure 3a, the adsorption isotherms are IUPAC type IV curves which identify the porosity as in the mesoporous range defined as between 2 and 50 nm according to the IUPAC convention. The hysteresis loop characterizing this type of isotherm is associated with capillary condensation of nitrogen in the mesopores. With increasing number of repeat units, n, plateaus at higher P/P_0 were observed, indicating a slight modification of the pore structures derived from longer polyimide oligomers. A graph of relative pore volume vs pore diameter is shown in Figure 3b for the same samples. From Figure 3b, it can be seen that the pore size distribution peaks around 25−40 nm (mesoporous) but trails out to about 100 nm (IUPAC convention defines macropore as >50 nm). Although the number of repeat units has little effect on the surface area, it does have a small effect on the pore size distribution. Aerogels formulated with $n = 25$ have a sharper pore size distribution with a peak at 26 nm. For aerogels formulated with $n = 15$, the pore size distribution is wider and the peak shifts to 40 nm.

Scanning electron micrographs (SEM) of the samples are shown in Figure 4. The samples do not look like silica aerogels, with the typical clusters or strings of particles. Rather, the polyimide aerogel morphology resembles bundles of polymer fibers tangled together with fiber diameters in the range of 15−50 nm. Also as seen in Figure 4, in agreement with the results

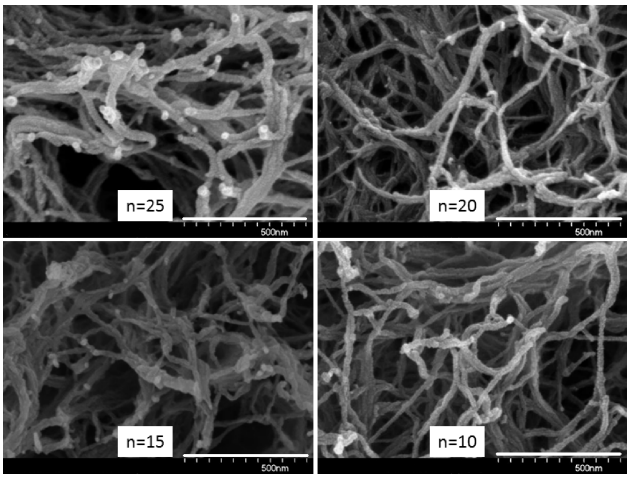

Figure 4. SEM images of OAPS cross-linked polyimide aerogels using oligomers of $n = 10$, $n = 15$, $n = 20$, and $n = 25$. The scale bars in the micrographs are all 500 nm.

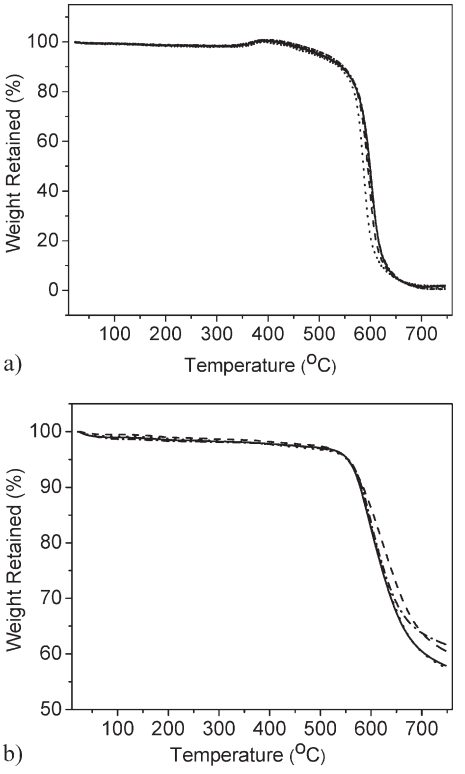

Figure 5. TGA of the samples in (a) air and (b) nitrogen, with OAPS cross-link and oligomers of $n = 25$ (solid line), $n = 20$ (dash-dotted line), $n = 15$ (dash line), and $n = 10$ (dotted line).

from the BET analysis, pore sizes can be seen ranging from mesoporous to as large as 200 nm and not much difference in the morphology can be detected between aerogels made using different n values.

Thermal gravimetric analysis (TGA) of the OAPS crosslinked polyimide aerogels was measured in both air and nitrogen from room temperature to 750 °C, and is shown in Figure 5. In both air and nitrogen, little weight loss occurs until the onset of decomposition at 560 °C, indicating that imidization is complete and NMP is removed efficiently by solvent exchange to acetone and

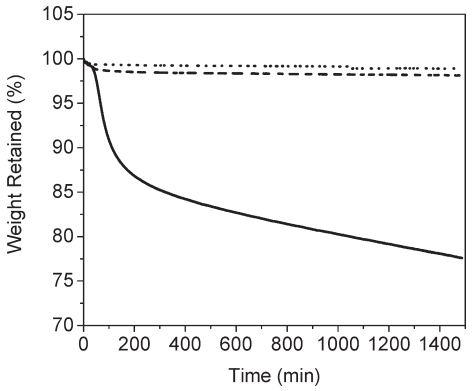

Figure 6. Isothermal TGA of OAPS cross-linked polyimide aerogel (n = 20) in nitrogen for 24 h at 300 °C (dotted line), 400 °C (dash line) and 500 °C (solid line).

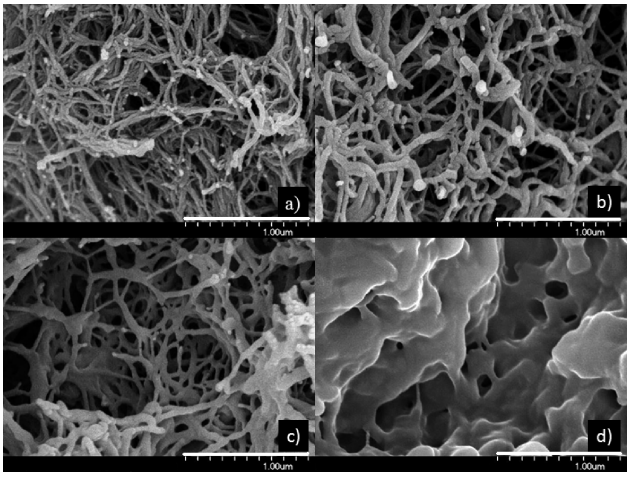

Figure 7. SEM images of the OAPS cross-linked polyimide aerogel (n = 20) at (a) room temperature and after heating for 24 h in nitrogen at (b) 300, (c) 400, and (d) 500 °C. The scale bars in the micrographs are all 1.00 μm.

supercritical drying. The TGA in air shows a weight increase with an onset of about 300 °C for all samples, which may be due to oxidation of the methylene groups from BAX to carbonyl, a typical oxidation pathway for the diphenylmethyl moiety in high-temperature polymers. There is little effect on the TGA curves due to the n value, with the exception of a slightly higher onset of degradation in nitrogen for aerogels produced from n = 25 oligomers.

Isothermal TGA of the samples was carried out at three different temperatures (300, 400, and 500 °C) in nitrogen for 24 h. Graphs of weight retention vs. time of the sample with n = 20, are shown in Figure 6. Weight loss at 300 °C (1%) and 400 °C (2%) after 24 h is quite low, suggesting short term use at these temperatures is possible. Indeed, SEM of samples after heating at 300 and 400 °C show little change. After 24 h at 500 °C, however, weight loss is 22.4% and as shown in Figure 7d, the mesoporous structure has collapsed.

Compression tests were performed on all aerogel formulations in the study and selected stress strain curves are shown in Figure 8a. The Young's modulus of the samples measured as the initial slope of the stress strain curve ranged from 1.7 MPa to 5.3 MPa. Previously studied polymer reinforced silica aerogels

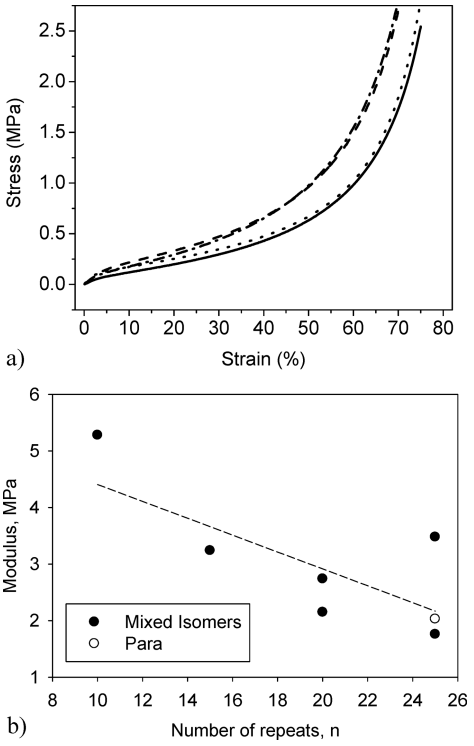

Figure 8. (a) Select stress−strain curves from compression of OAPS-polyimide aerogel at n = 10 (dotted line), n = 15 (dash line), n = 20 (dash-dotted line), and n = 25 (solid line); and (b) Young's modulus graphed vs number of repeat units, n.

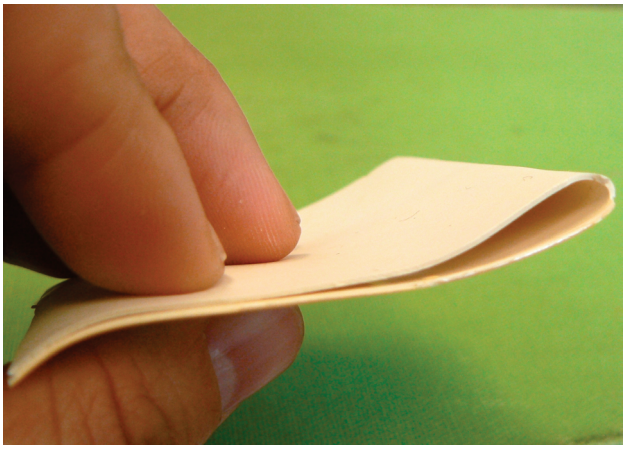

Figure 9. OAPS cross-linked polyimide aerogel thin film (n = 25).

with similar density have compressive modulus ranging from 0.1 to 2 MPa.[11−15] Hence, OAPS cross-linked polyimide aerogels have similar or higher modulus than typical polymer reinforced silica aerogels. As shown in Figure 8b, modulus decreases slightly as n is increased, despite the fact that density does not vary with n. Thus, this decrease in modulus must be due to the longer oligomer chains between OAPS cross-links. Also as shown in Figure 8b, aerogels made using *p*-OAPS are similar in modulus to those made using a mixture of isomers.

It is possible to cast thin films of OAPS cross-linked polyimide aerogels as shown in Figure 9. The thickness of the film is mainly determined by the casting Dr. Blade gap, the solution viscosity, casting speed and head pressure. With a casting speed of

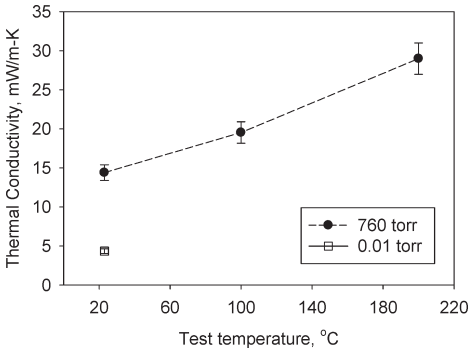

Figure 10. Thermal conductivity of OAPS cross-linked polyimide aerogels measured at different temperatures and pressures.

20 cm/min, a 6 in. wide Dr. Blade with a gap of 0.76 mm, the final film has a thickness of nominally 0.5 mm. Thin films made using $n = 25$ oligomers were very flexible. Lower n values result in more brittle films that crack when folded.

Polyimide aerogel films were tested for thermal physical properties between room temperature and 200 °C. Thermal diffusivity (a) values were measured in nitrogen gas at two different pressures (p = 760 Torr and 0.01 Torr) using the step heating (3P) method. Specific heating (Cp) values were determined using a differential scanning calorimeter. Thermal conductivity (λ) values were calculated using $\lambda = aCp\rho_b$, where ρ_b is the bulk density of the sample. Multiple thermal diffusivity measurements were made at each temperature and pressure level and average values are used to calculate thermal conductivity. At a pressure of 760 Torr and room temperature, thermal diffusity is measured to be 1.14×10^{-3} cm^2/s and drops an order of magnitude at 0.01 Torr to 3.4×10^{-4} cm^2/s.

Thermal conductivity plotted vs temperature is shown in Figure 10. Total relative expanded uncertainty ($k = 2$) of the thermal conductivity determination is ±7%. As seen in the graph, the polyimide aerogel has thermal conductivity of 14.4 mw/(m K) at room temperature and 760 Torr, similar to silica aerogels of the same density.[38] The thermal conductivity also increases with increasing temperature as expected and drops to 4.3 mW/(m K) at vacuum (0.01 Torr), which is also similar to that of the silica aerogel. Reducing the pressure lengthens the mean free path of the gas relative to the mean pore diameter, and there is a drop in thermal diffusivity and thus in the thermal conductivity.

CONCLUSIONS

A series of polyimide aerogels cross-linked using an aminophenyl decorated polysilsesquioxane, OAPS, was synthesized. The resulting aerogels have density ~0.1 g/cm^3, low shrinkage, high porosity (91−92%), and high surface area (240−260 m^2/g). With onset of decomposition of 560 °C, the aerogels are quite stable, losing only 1−2% weight on aging for 24 h at 300 and 400 °C. The polyimide aerogels have modulus as high as or higher than previously reported polymer reinforced silica aerogels, with similar thermal conductivity. In addition, thin films of the polyimide aerogels fabricated using $n = 25$ oligomers are quite flexible, making them suitable for use as an insulation layer for inflatable structures, such as decelerators for entry, descent and landing applications. Tensile properties and other characteristics of these films are currently under further investigation. In addition, structure property studies of polyimide formulations using different diamines and dianhydrides are also in progress.

AUTHOR INFORMATION

Corresponding Author

*E-mail: haiquan.n.guo@nasa.gov (H.G.); maryann.meador@nasa.gov (M.M.).

ACKNOWLEDGMENT

We gratefully acknowledge support from the Fundamental Aeronautics Program (Hypersonics). G.S. thanks the Interdisciplinary National Science Program Incorporating Research and Education Experience (INSPIRE) Project for support through a summer internship. We also thank Jozef Gembarovic from the Thermophysical Properties Research Lab, Inc. (TPRL), for measurement of thermal conductivity; Daniel Scheiman, ASRC, for carrying out porosimetry and thermal analysis; and Anna Palczer for nitrogen sorption experiments.

REFERENCES

(1) Kistler, S.S.; Caldwell, A. G. *Ind. Eng. Chem.* **1934**, *26*, 658–662.
(2) Hüsing, N.; Schubert, U. *Angew. Chem., Int. Ed.* **1998**, *37*, 22–45.
(3) Pierre, A. C.; Pajonk, G. M. *Chem. Rev.* **2002**, *102*, 4243–4265.
(4) Parmenter, K. E.; Milstein, F. *J. Non-Cryst. Solids* **1998**, *223*, 179–189.
(5) Moner-Girona, M.; Roig, A.; Molins, E.; Martínez, E.; Esteve, J. *J. Appl. Phys. Lett.* **1999**, *75*, 653–655.
(6) Moner-Girona, M.; Matinez, E.; Roig, A.; Esteve, J.; Molins, E. *J. Non-Cryst. Solids* **2001**, *285*, 244–250.
(7) Burchell, M. J.; Thomson, R.; Yano, H. *Planet. Space Sci.* **1998**, *47*, 189–204.
(8) Jones, S. M. *J. Sol−Gel Sci. Technol.* **2006**, *40*, 351–357.
(9) Leventis, N.; Sotiriou-Leventis, C.; Zhang, G.; Rawashdeh, A. M. *Nano Lett.* **2002**, *2*, 957–960.
(10) Capadona, L. A.; Meador, M. A. B.; Alunni, A.; Fabrizio, E. F.; Vassilaras, P.; Leventis, N. *Polymer* **2006**, *47*, 5754–5761.
(11) Meador, M. A. B.; Capadona, L. A.; McCorkle, L.; Papadopoulos, D. S; Leventis, N. *Chem. Mater.* **2007**, *19*, 2247–2260.
(12) Nguyen, B. N.; Meador, M. A. B.; Medoro, A.; Arendt, V.; Randall, J.; McCorkle, L.; Shonkwiler, B. *ACS Appl. Mater. Interfaces* **2010**, *2*, 1430–1443.
(13) Meador, M. A. B.; Fabrizio, E. F.; Ilhan, F.; Dass, A.; Zhang, G.; Vassilaras, P.; Johnston, J. C.; Leventis, N. *Chem. Mater.* **2005**, *17*, 1085–1098.
(14) Meador, M. A. B.; Weber, A. S.; Hindi, A.; Naumenko, M.; McCorkle, L.; Quade, D.; Vivod, S. L.; Gould, G. L.; White, S.; Deshpande, K. *ACS Appl. Mater. Interfaces* **2009**, *1*, 894–906.
(15) Meador, M. A. B.; Scherzer, C. M.; Vivod, S. L.; Quade, D.; Nguyen, B. N. *ACS Appl. Mater. Interfaces* **2010**, *2*, 2162–2168.
(16) Faysal Ilhan, U.; Fabrizio, E. F.; McCorkle, L.; Scheiman, D. A.; Dass, A.; Palczer, A.; Meador, M. A. B.; Johnston, J. C.; Leventis, N. *J. Mater. Chem.* **2006**, *16*, 3046–3054.
(17) Nguyen, B. N.; Meador, M. A. B.; Tousley, M. E.; Shonkwiler, B.; McCorkle, L.; Scheiman, D. A.; Palczer, A. *ACS Appl. Mater. Interfaces* **2009**, *1*, 621–630.
(18) Boday, D. J.; Stover, R. J.; Murighi, B.; Keller, M. W.; Wertz, J. T.; Obrey, K. A. D.; Loy, D. A. *ACS Appl. Mater. Interfaces* **2009**, *1*, 1364–1369.
(19) Braun, R. D.; Manning, R. M. *J. Spacecr. Rockets* **2007**, *44*, 310–323.
(20) Reza, S.; Hund, R.; Kustas, F.; Willcockson, W.; Songer, J. *19th AIAA Aerodynamic Decelerator Systems Technology Conference and Seminar*; Williamsburg, VA, May 21−24; American Institute of Aeronautics and Astronautics: Reston, VA, 2007; p 2007-2516.
(21) Wendall, R.: Wang, J.; Begag, R. U.S. Patent WO/2004/009673, Jan. 29, 2004.
(22) Chidambareswarapattar, C.; Larimore, Z.; Sotiriou-Leventis, C.; Mang, J. T.; Leventis, N. *J. Mater. Chem.* **2010**, *20*, 9666–9678 also

reports similar linear polyimide aerogels and a new polymer aerogel made from the reaction of 4,4′-methylenediphenyl di-isocyanate and pyromellitic dianhydride. The authors claim that the latter aerogel is cured at room temperature into a polyimide. However, the data do not support this assertion. The spectral data are somewhat ambiguous, but the reported thermal gravimetric analyses of the room temperature derived aerogels show a weight loss at 200 °C of about 7−8%. This would be the expected weight loss due to water during imide formation from polyamic acid that typically occurs at this temperature. In any case, this type of polyimide should not lose weight at this temperature.

(23) Kawagishi, K.; Saito, H.; Furukawa, H.; Horie, K. *Macromol. Rapid Commun.* **2007**, *28*, 96–100.

(24) Meador, M. A. B.; Malow, E. J.; He, Z. J.; McCorkle, L.; Guo, H.; Nguyen, B. N. *Polym. Prepr.* **2010**, *51*, 265–266.

(25) Tarmaki, R.; Tanaka, Y.; Asuncion, M. Z.; Choi, J.; Laine, R. M. *J. Am. Chem. Soc.* **2001**, *123*, 12416–12417.

(26) Waddon, A. J.; Coughlin, E. B. *Chem. Mater.* **2003**, *15*, 4555–4561.

(27) Wright, M. E.; Schorzman, D. A.; Feher, F. J.; Jin, R.-Z. *Chem. Mater.* **2003**, *15*, 264–268.

(28) Mather, P. T.; Jeon, H. G.; Romo-Uribe, A. *Macromolecules* **1999**, *32*, 1194–1203.

(29) Strachota, A.; Kroutilová, I.; Kovářová, J.; Matějka, I. *Macromolecules* **2004**, *37*, 9457–9464.

(30) Lee, Y.-J.; Huang, J.-M.; Kuo, S.W.; Chang, F.-C. *Polymer* **2005**, *46*, 10056–10065.

(31) Huang, J.; Lim, P.C.; Shen, L.; Pallathadka, P.K.; Zeng, K.; He, C. *Acta Mater.* **2005**, *53*, 2395–2404.

(32) Huang, J.-C.; He, C.-B.; Xiao, Y.; Mya, K. Y.; Dai, J.; Ping Siow, Y. *Polymer* **2003**, *44*, 4491–4499.

(33) Tamaki, R.; Choi, J.; Laine, R. M. *Chem. Mater.* **2003**, *15*, 793–797.

(34) Liu, Y.; Wang, Z.; Li, G.; Ding, M. *High Perform. Polym.* **2010**, *22* (1), 95–108.

(35) Kinsman, D.; Kagumba, L.; Gavrin, A.; Rice, N.; Meador, M. A.; Scheiman, D. A. *International SAMPE Symposium and Exhibition*; Society for the Advancement of Material and Process Engineering: Covina, CA, 2002; Vol. 47, pp 395−403.

(36) Gembarovic, J.; Taylor, R.E. *Int. J. Thermophys.* **2007**, *28*, 2164–2175.

(37) Barton, T.J.; Bull, L. M.; Klemperer, W. G.; Loy, D. A.; McEnaney, B.; Misono, M.; Monson, P.A.; Pez, G.; Scherer, G. W.; Vartuli, J. C.; Yaghi, O. M. *Chem. Mater.* **1999**, *11*, 2633–2656.

(38) Reichenauer, G.; Heinemann, U.; Ebert, H.-P. *Colloids Surf., A* **2007**, *300*, 204–210.